

# TURBULENCE MEASUREMENTS IN THE BOUNDARY LAYER OVER A STREAMWISE EDGE (CHINE)

Panchapakesan, N. R. and P.N. Joubert.

Department of Mechanical and Manufacturing Engineering  
University of Melbourne, Parkville VIC 3052, Australia.

## ABSTRACT

The turbulent boundary layer developing over a chine aligned with the flow provides a sufficiently complex three dimensional flow that include many of the mechanisms seen in turbulent flows encountered in practice. In this paper we present mean flow measurements and some turbulence measurements characterizing the evolution of the boundary layer in this simple geometry. The measurements indicate the presence of stress induced secondary flows as expected from studies in related geometries. The mean flow is seen to be asymmetric with respect to the corner bisector. This asymmetry is also seen to influence the turbulence field.

## INTRODUCTION

Turbulent boundary layers that develop over airplanes and ships and in turbomachines are in general three dimensional. They are greatly influenced by the extra-strain rates (i.e. other than that due to the gradient of the streamwise velocity normal to the wall) that are invariably present in these flows. A series of experiments investigating the effects of extra-strain rates on the development of turbulent boundary layers have been completed at the University of Melbourne. Saddinghi & Joubert studied the effects of lateral divergence on an initially two dimensional turbulent boundary layer. Panchapakesan et. al. studied the effects of lateral convergence. Hard chines, which are edges formed at the intersection of two surfaces, are found in the geometry of many transport vehicles notably in ship hulls. The turbulent boundary layer that develops over such a geometry is a slender three dimensional one with non-negligible gradients in directions transverse to

the streamwise direction. The streamwise edge or the external corner at the intersection of two plane surfaces at right angles is a simple representative of the chines found in practice. It is this geometry that is investigated here as a flow next in complexity to the earlier studies cited.

Flow past the lateral edge of a finite flat plate aligned with the streamwise direction has been studied by Davies & Young and Elder. Elder also studied the flow past bars of small aspect ratios. Brief description of their work may be found in Townsend's text book (section 7.19). Another related flow configuration is that along an internal corner which has been studied as both a homogeneous flow in a duct (see for e.g. Brundrett & Baines) and as an unconfined developing flow along an internal corner (Mojola & Young). In all these configurations the anisotropy of the turbulence near the wall together with the transverse gradients that arise due to the presence of the edge or the corner generate a secondary mean flow and produce mean streamwise vorticity (see Bradshaw).

The geometries investigated by Elder, viz. lateral edge of a finite flat plate and small aspect ratio bars aligned with the flow, are the ones that are most relevant to our investigation. He used a pitot tube to measure the velocity field and calculated wall shear stresses. He also used a vortameter to deduce the nature of the secondary flow. The characterization of the turbulence field in the flow over the chine is our primary goal and this complements Elder's work.

## EXPERIMENTAL APPARATUS & TECHNIQUES

The test section in which the experiments were con-

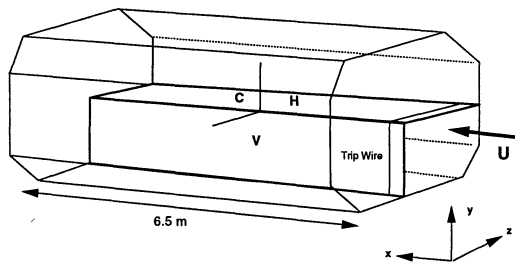


Figure 1: Schematic diagram of the test section with the chine.

ducted is shown schematically in Figure 1. The octagonal shape of the cross-section fits inside a rectangle of sides 1.3 m by 1.68 m. The test section is constructed from aluminium slats with narrow gaps between them. The blockage effect of the models used in the test section is minimized by this construction. A large closed circuit wind tunnel supplies the test section with wind. Two plane surfaces made from varnished medium density fibre boards of half test section widths and running its entire length make up the chine. Aluminium airfoils of a symmetric section were attached to the leading edges to avoid separation. The boundary layers were tripped with stainless steel wires of 1.2 mm size fixed to the boards about 80 mm from where the aluminium airfoil and the chine boards meet. The trip wire was taken as the reference for axial distance measurements and the corner for transverse distances.

The measurements were made with a nominal tunnel speed of about 10 m/s corresponding to a unit Reynolds number of  $6.8 \times 10^5$  per metre. Measurement traverses were made in regions close to the corner over the horizontal (H) and vertical (V) boards and in the corner region (C). In the corner region the traverses were along radial lines at 15 degree intervals covering the 90 degree region. Five axial locations at  $x = 0.17, 1.19, 2.25, 3.49, 4.67$  m were chosen for measurement traverses. A boundary layer pitot tube with a 0.7 mm dynamic head tube and a separate static pressure tube was used for mean velocity traverses. A single wire hot-wire probe was used for turbulence measurements. We present some of the measurements at the farthest axial location of 4.67 m. in this paper and provide a partial characterization of the flow. Detailed cross-wire measurements are currently under way and a more complete analysis of the flow based on those measurements will be presented subsequently.

## RESULTS & DISCUSSION

The axial variation of the boundary layer thicknesses derived from pitot tube traverses is shown in figure 2. The farthest measurement outside the region of influence of the corner is taken to be the 2-D value. The measurements are compared with those of Erm (1988) and Marusic (1991) taken in similar boundary layers at

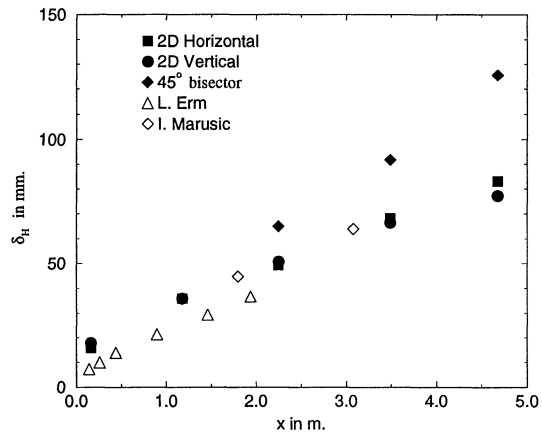


Figure 2: Axial variation of boundary layer thicknesses.

the same unit Reynolds number. The boundary layer away from the corner can be seen to be developing as a 'standard' two-dimensional boundary layer. Calculation of the wake factor from the measured velocity profiles and the Reynolds number based on the momentum thickness indicate that they fall very close to the Coles curve derived from empirical data for two-dimensional boundary layers.

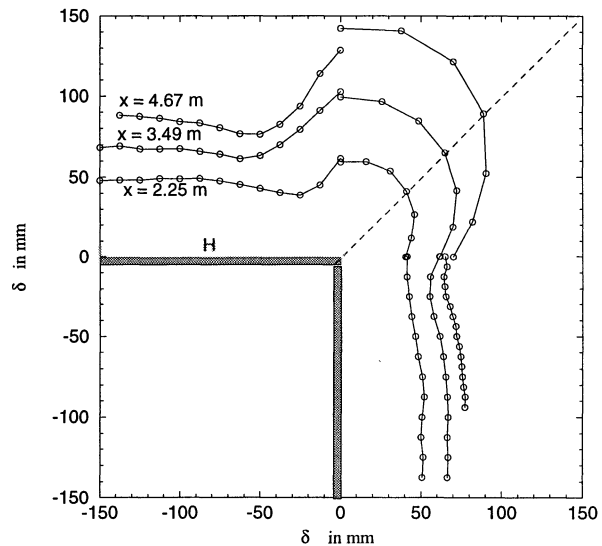


Figure 3: Lateral variation of boundary layer thickness.

The variation of the boundary layer thickness in the transverse directions for three measurement stations are shown in figure 3. The initial thinning of the boundary layer as we move from the two dimensional region towards the corner and a subsequent thickening due to the secondary flow was also observed by Elder in his measurements over the finite flat plate and rectangular section bars. This similarity indicates that the secondary flow in this case is away from the corner along the bisector and returns back into the boundary layer

towards the wall farther from the corner. The development of the boundary layer can be seen to be asymmetric with respect to the bisector at the corner. Measurements in the corner region have also been made at axial locations closer to the origin. At  $x = 0.17$  m the boundary layer is completely symmetric with velocity traverses along each radial traverses collapsing on top of each other. The asymmetry develops slowly beyond that and is perceptible at  $x = 1.19$  m.

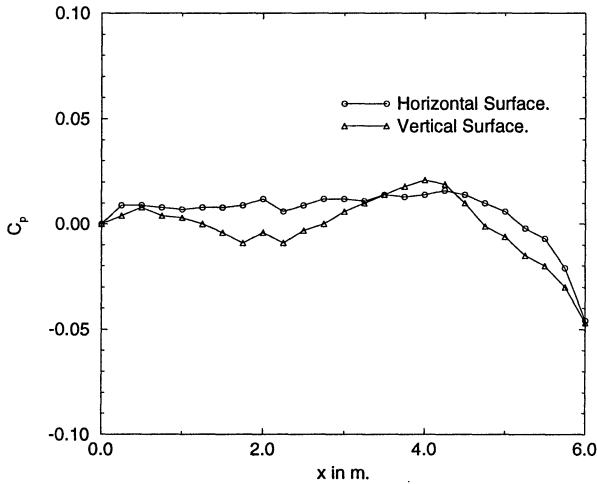


Figure 4: Longitudinal variation of  $C_p$ .

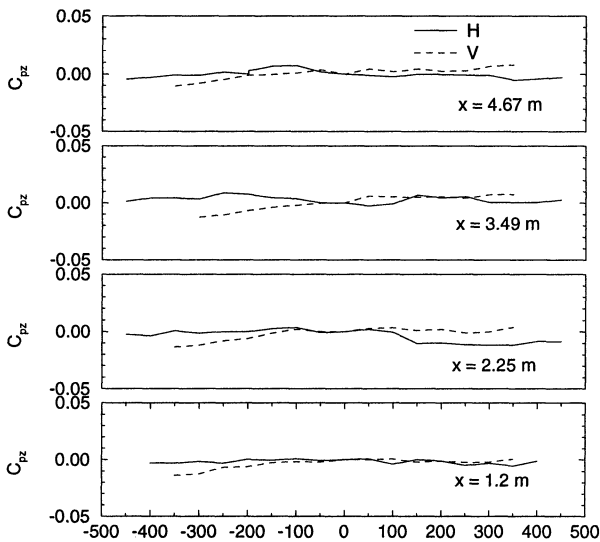


Figure 5: Transverse variation of  $C_p$ .

In order to ensure that the flow development is not affected by external flow conditions, the free stream velocities were measured at a height of 275 mm outside the boundary layer and along the centre of the two chine board surfaces. These velocities were converted to pressure coefficients and are presented in figure 4 with the velocity at the  $x = 0$  being taken as the reference value. At the very end of the test section where the test section

joins the tunnel structure there is a gap. The gap affects the free stream velocities close to the end of the test section. But, in the large region where measurements have been made (i.e.  $x = 0$  to 4.67 m) the  $C_p$  is well within  $+0.02$  and  $-0.01$ . Thus the effect of any longitudinal pressure gradient on flow development should be very small. Transverse variations of the free stream velocities, measured at a height of 275 mm above the two surfaces, at different streamwise locations converted to pressure coefficients are shown in figure 5. The values of  $C_p$  over much of the region where measurements have been made are within  $+0.01$  and  $-0.01$ . This indicates that the flow above the corner region is fairly homogeneous and the asymmetric development is unlikely to be caused by an external pressure gradient.

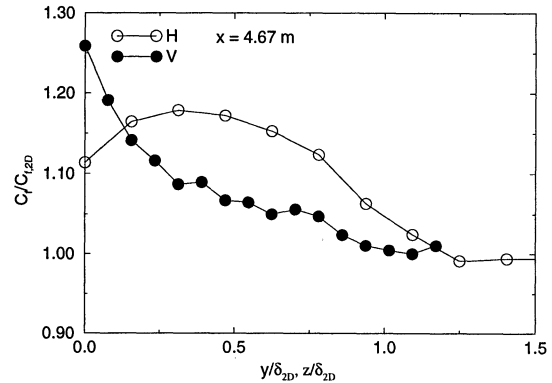


Figure 6: Lateral variation of skin friction coefficient.

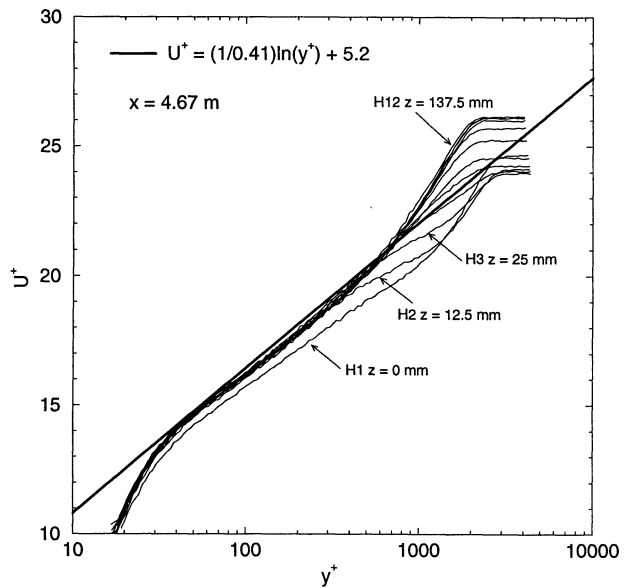


Figure 7: Mean velocity profiles over the horizontal surface.

The variation of the skin friction coefficient at the last axial location,  $x = 4.67$  m, is shown in figure 6. These values were calculated using the Preston tube

method from the measurement with a pitot tube at the wall. The measured values change sharply over the corner and the influence of the secondary flow is seen to be different on the two surfaces. The extent of the region of influence of the corner is of the order of one 2-D boundary layer thickness.

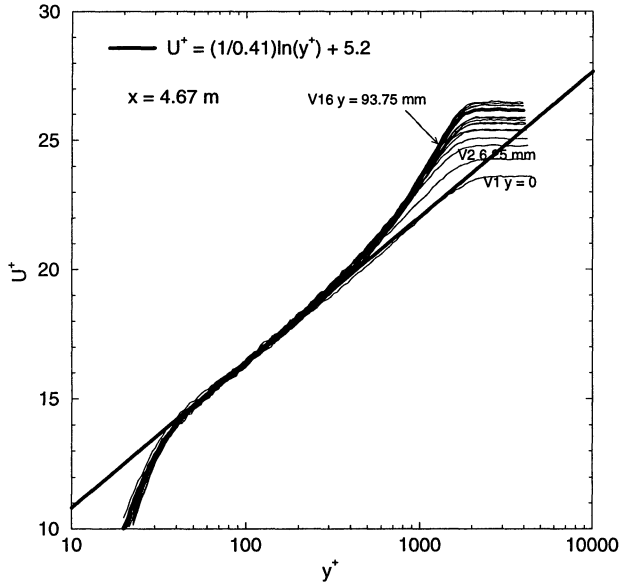


Figure 8: Mean velocity profiles over the vertical surface.

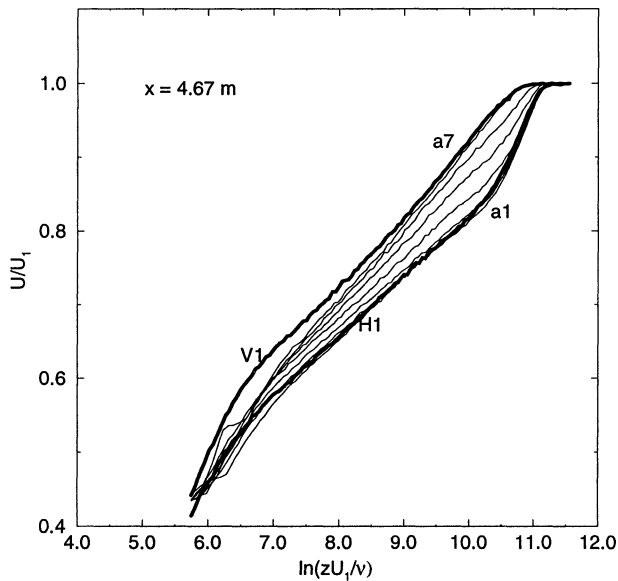


Figure 9: Mean Velocity profiles in the corner region.

The mean streamwise velocity and rms streamwise fluctuating velocity fields at the farthest axial location are shown in the subsequent figures. Figures 7 and 8 show the mean velocity field, plotted in wall coordinates, over the two chine surfaces. While the locations close to the corner cannot be expected to show

a log-law region, all other transverse locations show a clear logarithmic region as expected. The asymmetry of the flow with respect to the bisector is clearly seen in figure 9 where the flow continuously changes from that on one surface to the other.

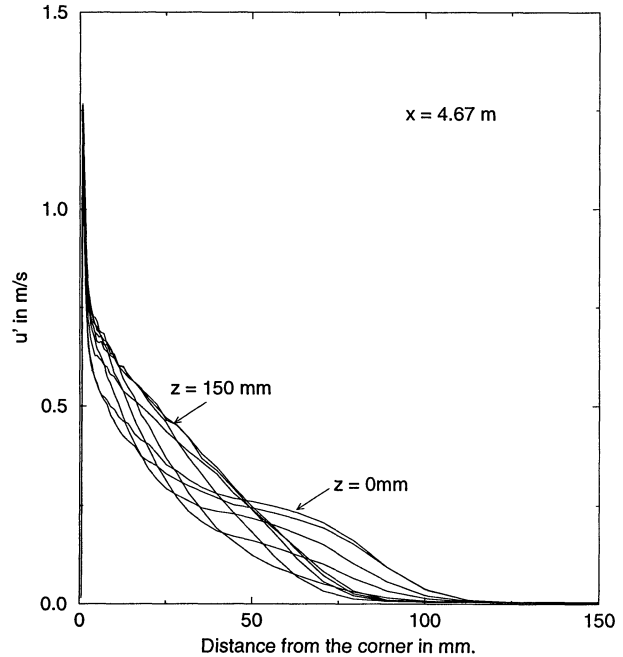


Figure 10: Turbulence intensity along the horizontal surface.

The intensities of turbulence fluctuations of the streamwise velocity fluctuations are shown in figures 10 through 12. Over the horizontal surface, as seen in figure 10, the turbulence close to the wall and near the corner is attenuated but is enhanced in the outer region in comparison with the 2-D profile of nearly linear variation seen far from the corner. Transport by the secondary flow is believed to be the primary mechanism, but a closer look at the values very close to the wall indicate that the secondary flow also affects the turbulence production near the corner. The profiles over the vertical surface show the effect of the asymmetric mean flow field on the turbulence. The turbulence is attenuated all through the boundary layer as we move towards the corner. Figure 12 shows the variation in the corner region changing from one state to the other. A more complete picture will emerge with cross-wire measurements of Reynolds stresses and calculation of energy balances.

## CONCLUSIONS

The mean flow measurements over the corner region of a chine presented here indicate that the influence of the corner is felt up to one or two boundary layer thick-

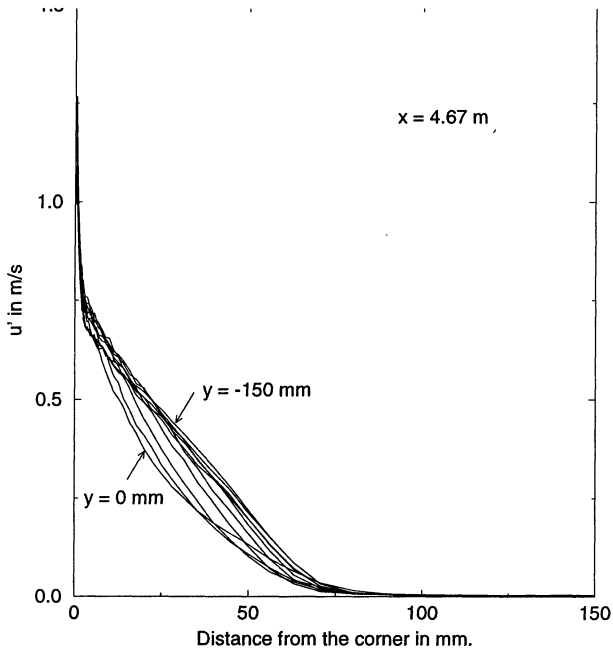


Figure 11: Turbulence intensity along the vertical surface.

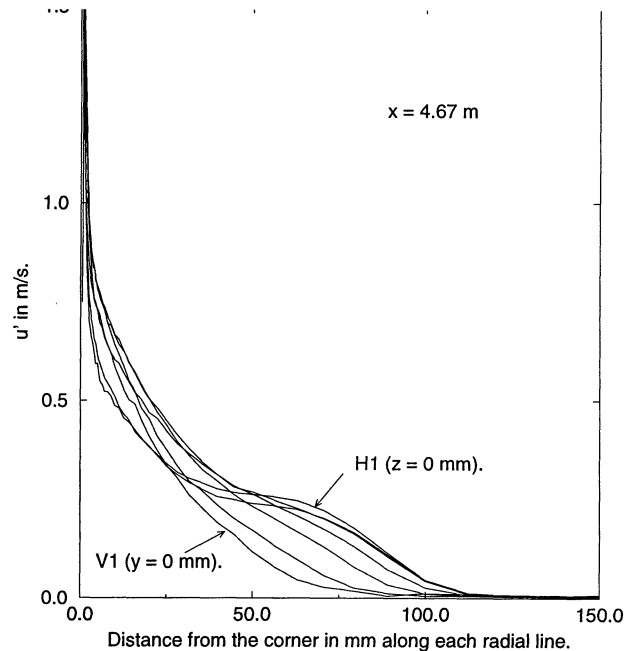


Figure 12: Turbulence intensity in the angular region.

nesses at that location. The nature of the secondary flow is consistent with measurements in other related geometries. The growth of the corner region is seen to be almost linear. It is not clear whether this rate will be sustained farther downstream. The asymmetry of the secondary flow with respect to the corner bisector is non-negligible and persistent.

## REFERENCES

- BRADSHAW, P., 1987. "Turbulent Secondary Flows." *Annual Review of Fluid Mechanics*, **19**, 53-74.
- BRUNDRETT, E. and BAINES, W.D., "The Production and Diffusion of Vorticity in a Duct Flow." *J. Fluid Mech.* **19** 375-394.
- DAVIES, E.B. and YOUNG, A.D., 1963. "Streamwise Edge Effects in the Turbulent Boundary Layer on a Flat Plate of Finite Aspect Ratio." *A.R.L.R. & M* 3367.
- ELDER, J.W., 1967. "The Flow Past a Flat Plate of Finite Width." *Journal of Fluid Mechanics*, **9**, 133-153, 1967.
- ERM, L.P., 1988. "Low Reynolds-number Turbulent Boundary Layers." *Ph.D. thesis, University of Melbourne, Australia.*
- MARUSIC, I., 1991. "The Structure of Zero- and Adverse-Pressure-Gradient Turbulent Boundary Layers." *Ph.D. thesis, University of Melbourne, Australia.*
- MOJOLA, O.O. and YOUNG, A.D., 1972. "An Experimental Investigation of the Turbulent Boundary Layer Along a Streamwise Corner." *AGARD CP 93*, 12.1-12.9.
- PANCHAPAKESAN, N.R. et. al., 1997. "Lateral

Straining of Turbulent Boundary Layers. Part 2. Streamline Divergence." *Journal of Fluid Mechanics*, **349**, 1-30.

SADDOUGHI, S.G., 1989. "Some selected contributions from Peter N. Joubert and his students to the study of perturbed turbulent boundary layers." *Tenth Australasian Fluid Mechanics Conference - University of Melbourne* 6.7-6.11.

SADDOUGHI, S.G. and JOUBERT, P.N., 1991. "Lateral Straining of Turbulent Boundary Layers. Part 1. Streamline convergence." *Journal of Fluid Mechanics*, **229**, 173-204.

TOWNSEND, A.A., 1976. "The Structure of Turbulent Shear Flow." *2nd Edition. Cambridge University Press.*